Photoexcited Electron Transfer: Short-Time Dynamics and Turnover Control by Dephasing, Relaxation, and Mixing

Guy Ashkenazi,[†] Ronnie Kosloff,*[,†] and Mark A. Ratner*[,‡]

Contribution from the Department of Physical Chemistry and Fritz Haber Institute for Molecular Dynamics, Hebrew University, Jerusalem, Israel, and Department of Chemistry, Northwestern University, Evanston, Illinois 60208

Received June 8, 1998. Revised Manuscript Received November 10, 1998

Abstract: In the usual parabolic, spin-boson approximation, understanding the dynamics of electron transfer reduces to following the coupled electron/vibration system throughout its exploration of the coupled potential energy surfaces. We discuss such an analysis for a very simple model for photoexcited electron transfer, consisting of two electronic states, one coupled vibration, and bath terms that describe solvent relaxation and dephasing. The current results are numerically exact. They correspond to the evolution of the system reduced density matrix, with relaxation and dephasing contributions from the environment. We observe control elements due to electronic and vibrational dephasing and relaxation, nonadiabatic coupling, and temperature. Many of these parameters exhibit a turnover phenomenon (nonmonotonic behavior of the rate change as the appropriate interaction strength varies). The onset of irreversible (rate-type) behavior, short time quantum beats, multiple time scales, and other characteristic phenomena appear clearly in this very simplified and reduced structural model. The differences between this full dynamical analysis and the very useful transition-state or equilibrium vibronic model arises from the nonequilibrium nature of the initial photoexcited state, whose decay is effected by dephasing and relaxation dynamics as well as energetics.

I. Introduction

Chemical dynamics is often concerned with the study of a molecular subsystem, whose evolution occurs within a weakly coupled, statistically dominant environment. Obvious examples include molecular isomerization or vibrational relaxation in solvents, collision phenomena in a bathing gas, and charge or energy transfer processes between electronic sublevels in a large molecule or solvent environment. The dynamical evolution of such systems, especially in photoexcited initial states, can now be studied with use of ultrafast methods that provide information about the onset of irreversible rate-type behavior, and about the short time relaxation processes and the nature of system excitations as a function of time (refs 1−31 are representative of recent work). Theoretically, while wave function methods can describe this phenomenon under particular sets of approximations,[1,32,33] an appropriate language is clearly that of

[†] Hebrew University.

[‡] Northwestern University.

(1) Bixon, M.; Jortner, J. *Adv. Chem. Phys.* In press.

(2) van Grondelle, R.; Dekker, J. P.; Gillbro, T.; Sundström, V. *Biochim. Biophys. Acta* **1994**, *1187*, 1. Pullerits, T.; Sundström, V. *Acc. Chem. Res.* **29**, *381*, 1996.

(3) Rosker, M. J.; Wise, F. W.; Tang, C. L. *Phys. Rev. Lett.* **1986**, *57*, 321.

(4) Zewail, A. H. *Femtochemistry*; World: Singapore, 1994.

(5) Barbara, P. F.; Fujimoto, J. G.; Mikrov, W. H.; Zinth, W., Eds. *Ultrafast Phenomena X*; Springer: New York, 1996.

(6) Banin, U.; Ruhman, S. *J. Chem. Phys.* **1992**, *98*, 4391.

(7) Dhar, L.; Rogers, J. A.; Nelson, K. A. *Chem. Rev.* **1994**, *94*, 157.

(8) Barbara, P. F.; Meyer, T. J.; Ratner, M. A. *J. Phys. Chem.* **1996**, *100*, 13148−13168.

(9) Barbara, P. F.; Walker, G. C.; Smith, T. P. *Science* **1992**, *256*, 975. Johnson, A. E.; Levinger, N. E.; Jarzeba, W.; Schlief, R. E.; Kliner, D. A. V.; Barbara, P. F. *Chem. Phys.* **1993**, *176*, 555.

(10) Reid, P. J.; Silva, C.; Barbara, P. F.; Karki, L.; Hupp, J. T. *J. Phys. Chem.* **1995**, *99*, 2609.

(11) Spears, K. G.; Wen, X.; Arrivo, S. M. *J. Phys. Chem.* **1994**, *98*, 9693.

(12) Yoshihara, K.; Tominaga, K.; Nagasawa, Y. *Bull. Chem. Soc. Jpn.* **1995**, *68*, 696.

(13) Wiederrecht, G. P.; Svec, W. A.; Niemczyk, M. P.; Wasielewski, M. R. *J. Phys. Chem.* **1995**, *99*, 8918.

(14) Miyasaka, H.; Tabata, A.; Kamada, K.; Mataga, N. *J. Am. Chem. Soc.* **1993**, *115*, 7335.

(15) Fleming, G. R.; VanGrondelle, R. *Phys. Today* **1994**, *47*, 48.

(16) Franzen, S. F.; Martin, J.-L. *Annu. Rev. Phys. Chem.* **1995**, *46*, 453.

(17) Michel-Beyerle, M. E.; Small, G. J.; Hochstrasser, R. M.; Hofacker, G. L. *Chem. Phys.* **1995**, *197*, 223 (Special issue). Michel-Beyerle, M. E. *The Reaction Center of Photosynthetic Bacteria*; Springer: Berlin, 1995.

(18) Thompson, P. A.; Simon, J. D. *J. Am. Chem. Soc.* **1993**, *115*, 5657.

(19) Poellinger, F.; Heitele, H.; Michel-Beyerle, M. E.; Anders, C.; Futscher, M.; Stabb, H. A. *Chem. Phys. Lett.* **1992**, *198*, 645.

(20) Doorn, S. K.; Dyer, R. B.; Stoutland, P. O.; Woodruff, W. H. *J. Am. Chem. Soc.* **1993**, *115*, 6398. Wang, C.; Walker, G. C. *J. Am. Chem. Soc.* In press.

(21) Rossky, P. J.; Simon, J. D. *Nature* **1994**, *370*, 263.

(22) Tominaga, K.; Walker, G. C.; Kang, T. J.; Barbara, P. F. *J. Phys. Chem.* **1991**, *95*, 10485.

(23) Vos, M. H.; Rappaport, F.; Lambry, J.-C.; Treton, J.; Martin, J.-L. *Nature* **1993**, *363*, 320.

(24) Bradforth, S. E.; Jimenez, R.; Mourik, F. v.; Grondelle, R. v.; Fleming, G. R. *J. Phys. Chem.* **1995**, *99*, 16179. Joo, T.; Jia, Y.; Yoo, J.-Y.; Jonas, D. M.; Fleming, G. R. *J. Phys. Chem.* **1996**, *100*, 2399.

(25) Arnett, D. C.; Vöhringer, P.; Scherer, N. F. *J. Am. Chem. Soc.* **1995**, *117*, 12262. Wang, Q.; Schoenlein, R. W.; Peteanu, L. A.; Mathews, R. A.; Shank, C. V. *Science* **1994**, *266*, 422.

(26) Fleming, G. R.; Cho, M. *Annu. Rev. Phys. Chem.* **1996**, *47*, 109.

(27) Wynne, K.; LeCours, S. M.; Galli, C.; Therien, M. J.; Hochstrasser, R. M. *J. Am. Chem. Soc.* **1995**, *117*, 3729.

(28) Vos, M. H.; Jones, M. R.; Breton, J.; Lambry, J. C.; Martin, J.-L. *Biochemistry* **1996**, *35*, 2687.

(29) Wynne, K.; Hochstrasser, R. M. *Adv. Chem. Phys.* In press.

(30) Scherer, N. F.; Matro, A.; Ziegler, L. D.; Du, M.; Carlson, R. J.; Cina, J. A.; Fleming, G. R. *J. Chem. Phys.* **1992**, *96*, 4180. Scherer, N. F.; Jonas, D. M.; Fleming, G. R. *J. Chem. Phys.* **1993**, *99*, 153.

(31) Li, Z.; Zadoyan, R.; Apkarian, V. A.; Martens, C. C. *J. Phys. Chem.* **1995**, *99*, 7453.

(32) Bixon, M.; Jortner, J. *J. Chem. Phys.* ***1997***, *107*, 1470.

10.1021/ja981998p CCC: $18.00
Published on Web 03/27/1999

the reduced density matrix.[34−45] This is because one is concerned not with the study of pure states (that will involve the full dynamics of the molecular system plus bath, and is both computationally intractable and conceptually inappropriate), but rather with the discrete, observable substates that correspond to the molecule itself. Analysis of the subsystem in the presence of the dynamical bath variables is an important, very widely studied issue in current chemical dynamics research.[35−50]

Intramolecular electron transfer (ET) remains one of the most active subfields of chemical dynamics.[1,8,51−56] It is an exemplary situation for the study of subsystem evolution, since photoexcited initial electronic states decay to final, product states while sharing energy both between electronic and vibrational subsystems and between the molecule and its environment. The long time observable in such systems is generally a rate constant for ET, and standard theories of that rate constant[51−59] are almost always based on a model involving harmonic vibrations linearly coupled to two electronic states—that is, the spin-boson approximation.[53,60,61] Rate constants can be defined from such a model Hamiltonian either using activated complex theory or using a polaron type picture in which the rate constant is determined from the golden rule.[51,53] These treatments have proven extremely powerful in understanding ET reactions over many time scales, in many environments, and for many chemical situations.

If one is interested in short time behavior of such photoexcited ET systems, the situation becomes more complex. Many current ultrafast experiments[1−31] are indeed devoted to the onset of rate behavior, to the short time relaxation and dephasing dynamics of the initial state, to the time-dependent spectroscopic observation of the system, and to understanding how such important system parameters as temperature, frequency, electronic energy, coupling strength, and environmental interaction determine the evolution of the initial photoexcited state.

Because the dynamics of the system is inherently quantum mechanical, and because the dimensionality can be high, theoretical studies of the short time relaxation are generally performed with use of approximate methods for multimode systems. The approach that we take here is different: we investigate a very simplified reduced model, whose sub-system dynamics can be treated exactly by using full quantum dynamics, and whose interaction with the environment can be treated by using semi-group methods[62−71] that reasonably describe dephasing and relaxation effects. The study of such a simplified model clarifies some important concepts in short time intramolecular charge flow, including parametric dependence, onset of kinetic behavior, time scales, quantum beat phenomena, and energy flow. The photoexcited ET experiment directly probes both dynamical relaxation behavior and long-time ET kinetics. This paper is devoted to exact analysis of a simple model system that shows both the onset of relaxation and the rate process, and important energetic and dephasing effects on the kinetics.

We observe a number of important and striking behaviors, including situations in which relaxation never actually occurs, and several instances of turn-over behavior—that is, situations in which, upon increasing a particular parameter (coupling constant or relaxation time) nonmonotonic behavior of the transfer rate occurs. The behavior in which a finite time is required before the onset of an exponential or multiexponential decay is expected, on the basis of a very short-time analysis of the time-dependent Schrodinger equation, to occur generally.[72] The present study is intended to examine what factors determine this finite time, how the system evolves during it, and how the

(33) Zhu, L.; Widom, A.; Champion, P. *J. Chem. Phys.* **1997**, *107*, 2859.
(34) Schatz, G. C.; Ratner, M. A. *Quantum Mechanics in Chemistry*; Prentice-Hall: Englewood Cliffs, 1994; Chapter 11.
(35) Farrar, T. C.; Harriman, J. C. *The Reduced Density Matrix*; Farragut Press: Madison, 1993.
(36) Mukamel, S. *Principles of Nonlinear Optical Spectroscopy*; Oxford: 1995. Mukamel, S.; Yan, Y. *J. Phys. Chem.* **1991**, *95*, 1015. Okada, A.; Chernyak, V.; Mukamel, S. *J. Phys. Chem.* **1998**, *A102*,1241.
(37) A selection of papers on coherent phenomena occurs in: *Chem. Phys.* **1998**, *233*, No. *7*, 2. (*Coherence in Chemical Dynamics*; Ruhman, S., Scherer, N., Eds.).
(38) Jean, J. M.; Fleming, G. R. *J. Chem. Phys.* **1995**, *103*, 2092. Jean, J. M. *J. Chem. Phys.* **1996**, *104*, 5638. Jean, J. M. *J. Phys. Chem.* **1998**, *102*, 7549. Ben-Nun, M.; Levine, R. D.; Fleming, G. R. *J. Chem. Phys.* **1996**, *105*, 3035.
(39) Mak, C. H.; Egger, R. *Adv. Chem. Phys.* **1996**, *93*, 39. Lucke, A.; Mak, C. H.; Egger, R.; Ankerhold, J.; Stockburger, J.; Grabert, H. *J. Chem. Phys.* **1997**, *107*, 8397.
(40) Tang, J.; Lin, S. H. *Chem. Phys. Lett.* **1996**, *254*, 6.
(41) Banin, U.; Bartana, A.; Kosloff, R. *J. Chem. Phys.* **1994**, *101*, 8461.
(42) Wolfseder, B.; Domcke, W. *Chem. Phys. Lett.* **1996**, *259*, 113. Domcke, W.; Stock, G. *Adv. Chem. Phys.* **1997**, *100*, 1. Wolfseder, B.; Seidner, L.; Stock, G.; Domcke, W. *Chem. Phys.* **1997**, *217*, 775.
(43) Sim, E.; Makri, N. *Chem. Phys. Lett.* **1996**, *249*, 224. Sim, E.; Makri, N. *Comput. Phys. Commun.* **1997**, *99*, 335.
(44) Pollard, W. T.; Dexheimer, S. L.; Wang, Q.; Peteanu, L.; Shank, C. V.; Mathies, R. A. *J. Phys. Chem.* **1992**, *96*, 6147.
(45) Cao, J.; Minichino, C.; Voth, G. A. *J. Chem. Phys.* **1995**, *103*, 1391. Hernandez, R.; Voth, G. A. *Chem. Phys.* **1998**, *233*, 243.
(46) Song, X.; Stuchebrukhov, A. A. *J. Chem. Phys.* **1993**, *99*, 969.
(47) Tully, J. C. *J. Chem. Phys.* **1990**, *93*, 1061.
(48) Pollard, W. T.; Felts, A. K.; Friesner, R. A. *Adv. Chem. Phys.* **1996**, *93*, 77.
(49) Webster, F.; Wang, E. T.; Rossky, P. J.; Friesner, R. A. *J. Chem. Phys.* **1994**, *100*, 4835. Bittner, E. J.; Rossky, P. *J. Chem. Phys*. **1997**, *107*, 8611.
(50) Hammes-Schiffer, S. *J. Chem. Phys.* **1996**, *105*, 2236.
(51) Bixon, M.; Jortner, J., Eds. *Adv. Chem. Phys.* Special Volumes on Electron Transfer, in press.
(52) Newton, M. D. *Chem. Rev.* **1991**, *91*, 767.
(53) Schatz, G. C.; Ratner, M. A. *Quantum Mechanics in Chemistry*; Prentice Hall: Englewood Cliffs, NJ, 1993; Chapter 10.
(54) Bolton, J. R.; Mataga, N.; McLendon, G. L., Eds. *Electron Transfer in Inorganic, Organic and Biological Systems*, American Chemical Society: Washington, DC, 1991.
(55) Marcus, R. A. *Rev. Mod. Phys.* **1993**, *65*, 599. Marcus, R. A. *J. Chem. Phys.* **1965**, *43*, 679. Hush, N. S. *Trans. Faraday Soc.* **1961**, *57*, 557.
(56) Special issue on Electron Transfer: *Chem. Phys.* **1993**, *176*, 289.
(57) Newton, M. D.; Sutin, N. *Annu. Rev. Phys. Chem.* **1984**, *35*, 437. Marcus, R. A.; Sutin, N. *Biochim. Biophys. Acta* **1985**, *811*, 265. Mikkelsen, K. V.; Ratner, M. A. *Chem. Rev.* **1987**, *87*, 113.
(58) Bixon, M.; Jortner, J. *Faraday Discuss. Chem. Soc.* **1992**, *74*, 171. Wiersma, D. A., Ed. *Femtosecond Reaction Dynamics*; North-Holland: Amsterdam, 1994.
(59) Ulstrup, J. *Charge-Transfer Processes in Condensed Media, Lecture Notes in Chemistry*; Springer-Verlag: New York, 1979; Vol. 10.
(60) Leggett, A. J.; Chakravarty, S.; Dorsey, A. T.; Fisher, M. P. A.; Garg, A.; Zwerger, W. *Rev. Mod. Phys.* **1987**, *59*, 1.
(61) Tanimura, Y.; Wolynes, P. G. *J. Chem. Phys.* **1992**, *96*, 8485. Bixon, M.; Jortner, J.; Cortes, J.; Heitele, H.; Michel-Beyerle, M. E. *J. Phys. Chem.* **1994**, *98*, 7289.
(62) Lindblad, G. *Commun. Math. Phys.* **1976**, *119*, 48.
(63) Gorini, V.; Kossokowski, A.; Sudarshan, E. C. G. *J. Math. Phys.* **1976**, *17*, 821.
(64) Alicki, R.; Landi, K. *Quantum Dynamical Semigroups and Applications*; Springer: Berlin, 1987.
(65) Kosloff, R.; Rice, S. A. *J. Chem. Phys.* **1980**, *72*, 4591.
(66) Kosloff, R. *Physica* **1982**, *110A*, 346. Kosloff, R.; Ratner, M. A. *J. Chem. Phys.* **1982**, *77*, 2841.
(67) Davies, E. B. *Quantum Theory of Open Systems*; Academic: New York, 1976.
(68) Geva, E.; Kosloff, R.; Skinner, J. L. *J. Chem. Phys.* **1995**, *102*, 8541.
(69) Kohen, D.; Marston, C. C.; Tannor, D. *J. Chem. Phys.* **1997**, *107*, 5236.
(70) Davis, W. B.; Kosloff, R.; Ratner, M. A.; Wasielewski, M. *J. Phys. Chem*. Submitted for publication.
(71) Kosloff, R.; Ratner, M. A.; Davis, W. B. *J. Chem. Phys.* **1997**, *106*, 7036.
(72) Evans, D. G.; Nitzan, A.; Ratner, M. A. *J. Chem. Phys.* In press. Coalson, R. D.; Evans, D. G.; Nitzan, A. *J. Chem. Phys.* **1994**, *101*, 436. Reimers, J. R.; Hush, N. S. *Chem. Phys.* **1989**, *134*, 323. Neria, A.; Nitzan, A. *Chem. Phys.* **1994**, *183*, 351.

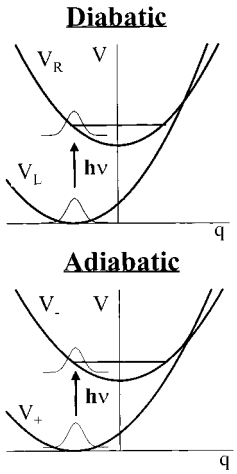

Figure 1. The potential energy curves used in the current analysis for electron transfer. The upper figures show diabatic curves that correspond to the eigenstates of the nuclear potential energy. The lower figure shows the adiabatic curves that include the electronic tunneling. Parameters are from Appendix 1.

subsequent rate process is controlled by dynamical, thermal, and dissipative interactions.

The formal structure of the model and the treatment of system/bath interactions are described in Section II. Actual results are discussed in Section III, and some remarks are made in the concluding section.

II. The Model and Its Analysis

Since the aim of the current paper is to discuss exact results for the curve crossing/electron transfer reaction, it is necessary to work in a model sufficiently simple that exact results can indeed be obtained. We will, therefore, represent the dynamical system in terms of the usual crossed parabolas of Figure 1. The overall Hamiltonian then consists of the electronic energy in either of the diabatic states, the vibrational energy associated with that diabatic state, and a crossing term that describes the passage for one parabolic well to the other. We work in a diabatic representation, so that the system molecular Hamiltonian can be written

$$H_s = |R\rangle\langle R|V_R(q) + |L\rangle\langle L|V_L(q) + (|R\rangle\langle L| + |L\rangle\langle R|)J \quad (1a)$$

The Hamiltonian as written involves only one vibrational

$$H_s = |R\rangle\langle R|\left\{\frac{P^2}{2M} + \frac{1}{2}M\omega^2(q - Q_0)^2\right\} + |L\rangle\langle L\left\{\frac{P^2}{2M} + \frac{1}{2}M\omega^2q^2 + \Delta\right\} + (|R\rangle\langle L| + |L\rangle\langle R|)J \quad (1b)$$

coordinate, whose equilibrium positions in reactant and product differ by the constant Q_0. The vibrational frequency is assumed the same for both electronic states, and is given by $\omega = (f/M)^{1/2}$; therefore, the innershell reorganization energy, or polaron stabilization energy, is given by

$$\lambda = \frac{1}{2}fQ_o^{\,2} \equiv S\hbar\omega \quad (2)$$

In these equations, λ represents the reorganization energy term, f is the force constant, M is the reduced mass of the vibrational degree of freedom, Δ is the exoergicity ($\Delta < 0$), and S is the dimensionless reorganization energy, or Huang−Rhys factor.[73,74]

The terms in the molecular Hamiltonian of eq 1 are respectively the electronic energy in the right potential well (corresponding to the photoexcited state), the electronic energy in the left well (the unexcited state before photoexcitation), and the diabatic mixing between the two states. This mixing is assumed (Condon approximation) to be a constant independent of nuclear position.

We describe the evolution of a molecule, characterized by the Hamiltonian of eq 1 and interacting with the solvent that causes phase relaxation and energy flow in the molecular subsystem. Formally, one can then write the total Hamiltonian in the usual way as

$$H = H_S + H_B + H_{SB} \quad (3)$$

where the subscripts S and B refer to the system and bath, respectively. Making a Markov density approximation (equivalently, assuming that the states of the system do not significantly perturb the states of the bath), we can write the reduced system density matrix as[34−36]

$$\sigma(x,q) = \mathrm{Tr}_B\{\rho(x,q,\vec{R})\} \quad (4)$$

Here σ and ρ are respectively the system reduced density matrix and the total density matrix. The coordinates x, q, and $\vec{R}$ are respectively the electronic coordinate, the intramolecular vibration, and the coordinates of the bath.

Because of the interaction between the system and the bath, the evolution of the system density matrix is affected by the energetics and dynamics of the bath degrees of freedom. Characterizing this interaction exactly is extremely challenging; characterizing it numerically requires demanding simulation.[72] For the purposes of our very simple model, we will assume that the effect of the system on the bath can be described by using the semigroup formalism.[62−71] This arises from a Markovian assumption (that the bath memory time is extremely short compared to any other appropriate time within the system). Under these conditions, and assuming a generalized interaction proportional to a sum of system operators times bath operators, the semigroup formalism permits a description of the time evolution of the system density matrix as

$$\dot{\sigma} = \frac{1}{i\hbar}[H_s,\sigma] + \dot{\sigma}\Big)_d \quad (5)$$

Here the first term on the right is the causal, Hamiltonian evolution of the system density matrix due to the system Hamiltonian. The second term on the right, the dissipative term, describes the dephasing and relaxation effects that the system encounters due to its interaction with the bath. The semigroup formalism for describing this interaction is described in detail elsewhere;[62−71] for current purposes, the presence of the bath manifests itself in three extra terms. These extra terms are vibrational dephasing and relaxation and electronic dephasing, all within the system.

The process of dephasing corresponds physically to fluctuations in the values of the system energies—electronic dephasing is then fluctuation in the electronic energy levels and vibrational dephasing describes changes in the vibrational energies. Obvious sources of dephasing are changes in the molecular solvent

(73) Huang, K.; Rhys, A. *Proc. R. Soc. London A* **1950**, *204*, 406.
(74) Jortner, J. *J. Chem. Phys.* **1976**, *64*, 4860.

environment or structure; all of these arise from the bath, and change the time evolution of the molecular states.

Formally, it is convenient to introduce a spin description of the crossed parabola model of eq 1. Then the model can be described as a spin-boson picture, and the system population levels can be replaced by those of a fictitious spin. Then the populations and transitions within the system are related to the spin variables by

$$2S_x = |R\rangle\langle L| + |L\rangle\langle R|$$

$$2S_y = i\{|R\rangle\langle L| - |L\rangle\langle R|\}$$

$$2S_z = |L\rangle\langle L| - |R\rangle\langle R|$$

$$S_\pm = S_x \pm iS_y \tag{6}$$

Here the operators S_+, S_-, and S_z are the usual spin operators that obey the commutation relations

$$[S_x,S_y] = iS_z$$

$$[S_+,S_z] = -S_+$$

$$[S_-,S_z] = S_-$$

$$[S_+,S_-] = 2S_z \tag{7}$$

The Hamiltonian of eq 1 can then be rewritten as (choosing as energy origin $(E_L + E_R)/2 = 0$, and letting I represent the unity operator).

$$H_s = (E_L - E_R)S_z + 2JS_x + \frac{P^2}{2M}I + \frac{f}{2}\left(\frac{1}{2}I + S_z\right)\left(q + \frac{Q_o}{2}\right)^2 + \frac{f}{2}\left(\frac{1}{2}I - S_z\right)(q - Q_o/2)^2 \tag{8}$$

The bath in which the molecule evolves will generally be a liquid solvent or a solid matrix. We will assume (phenomenologically) that the bath causes both relaxation and dephasing in the system, so that the reduced density matrix σ, which specifies the behavior of the electronic state and one vibrational mode, acquires new time-dependent relaxation and dephasing components. Their formal derivation is given elsewhere.[62−71] If we assume that the bath couples to the nuclear displacement (q) and to the electronic polarization (S_z), the semigroup formalism yields:

$$\dot{S}_x)_{ed} = -\gamma_{el}S_x$$

$$\dot{S}_y)_{ed} = -\gamma_{el}S_y$$

$$\dot{S}_z)_{ed} = 0 \tag{9a}$$

$$\dot{q})_d = \frac{-1}{2}(\gamma_{nd} + \gamma_{nr})q$$

$$\dot{p})_d = \frac{-1}{2}(\gamma_{nd} + \gamma_{nr})p \tag{9b}$$

$$\frac{d}{dt}\left(\frac{p^2}{2M} + \frac{M\omega^2}{2}q^2\right)_d = -\gamma_{nr}\left(\frac{p^2}{2M} + \frac{M\omega^2}{2}q^2\right) + k_{up}\hbar\omega \tag{9c}$$

The requirement for thermal equilibration of the vibration gives $k_{up}/k_{down} = \exp\{-\hbar\omega/k_BT\}$, and we define $k_{down} - k_{up} \equiv \gamma_{nr}$.

Here the parameters γ_{ed}, γ_{nd}, and γ_{nr} are respectively the rate parameters for electronic dephasing, nuclear dephasing, and nuclear relaxation. They are positive constants, whose magnitude will depend on the actual coupling between the system and the bath.

The overall equations of the system, then, can be written based on eqs 5, 8, and 9. It is these equations that can be solved exactly by using the quantum propagation scheme.

The actual density matrix propagation is described in detail elsewhere.[75] The main point is that the numerical procedure has exponential convergence. As a result the accuracy can be arbitrarily high, providing numerically exact results.

The analysis of the data can be presented in many ways, since the full density matrix in the electronic space and the space of the single vibrational coordinate is obtained. Similarly, the initial states must be specified both in the electronic two-level space and in the vibrational coordinate. We will assume that the initial situation corresponds to a photoexcitation, by one ultrafast pump pulse, from the ground state (left parabola) to the excited state (right parabola). We will limit our discussion to a situation in which the initial vibrational function is the ground state harmonic oscillator eigenstate (a simple Gaussian) promoted to the excited state. Generalization to more complex forms is possible, but our emphasis is on the dynamical evolution of the initially prepared state, rather than the details of that state. Similarly, we will ignore subsequent interactions between the electromagnetic field and the system. While such interactions are responsible both for important experimental effects (such as impulsive stimulated Raman scattering[76]) and for interesting aspects of molecular control (pulse field shaping of eigenstates,[77] laser cooling[78]), the emphasis here is really on the study of electron-transfer (ET) processes.

III. Results: Dynamical Evolution, Relaxation, Recurrences, and Rate Behavior

Traditional ET reactions are characterized by a rate constant—that is, they are concerned with the regime in which decay dynamics is exponential in time.[51−59] Contemporary ultrafast and pump/probe spectroscopies are concerned with the initial short-time behavior (subpicosecond regime), in which processes of relaxation and dephasing establish the conditions for first-order decay kinetics. Our analysis permits some understanding, based on the exact calculation of the model system, both of the initial short-time dynamics, and of the dependence of the eventual decay behavior both on the parameters of the system itself and on the system/bath coupling.

The first term in eq 5 for time evolution of the photoexcited system is fixed by the Hamiltonian parameters M (reduced mass of the oscillator), ω (oscillator frequency), Δ (exoergicity), Q_o (geometry change), and J (electron tunneling matrix element). The dissipative part (second term in eq 5) is described by the temperature T and the parameters γ_{nr}, γ_{nd}, and γ_{ed}. The model

(75) Berman, M.; Kosloff, R.; Tal-Ezer, H. *J. Phys.* **1992**, *A25*, 1283.
(76) Johnson, A. E.; Myers, A. B. *J. Chem. Phys.* **1996**, *104*, 2497. Jonas, D. M.; Bradforth, S. E.; Passino, S. A.; Fleming, G. R. *J. Phys. Chem.* **1995**, *99*, 2594. Ashkenazi, G.; Banin, U.; Bartana, A.; Kosloff, R.; Ruhman, S. *Adv. Chem. Phys.* **1997**, *100*, 229.
(77) Kosloff, R.; Rice, S. A.; Gaspard, P.; Tersigni, S.; Tannor, D. *Chem. Phys.* **1989**, *139*, 201. Weinacht, T. C.; Alm, J.; Buchsbaum, P. H. *Phys. Rev. Lett.* Submitted for publication.
(78) Bartana, A.; Kosloff, R.; Tannor, D. *J. Chem. Phys.* **1997**, *106*, 1435. Chu, S. *Science* **1991**, *253*, 861.

that we examine has been chosen to correspond very roughly to the energetics of the binuclear species $(NC)_5RuCNRu(NH_3)_5^-$. The parameter values are given in Appendix 1.

A. Short Time Behavior: The Onset of First-Order Kinetics. First-order kinetics require the existence of a dense set of levels, so that recurrences do not obtain. In the model analyzed here, these dense packed states do not occur specifically, but their role is taken by the dissipative terms in eq 5. In an actual physical system, all of the dissipation terms in eq 9 occur, but for analysis it is simplest to examine them individually.

1. No dephasing or relaxation (the Jaynes−Cummings model):[79] When all the dissipative terms of eq 5 are absent, the model becomes a two-level system coupled to a harmonic oscillator. This model was introduced by Jaynes and Cummings in the study of optical behavior. Because the states are now discrete and widely separated, no irreversible behavior occurs. Figure 2a shows the behavior of this Jaynes−Cummings model over the first 15 ps. The time scale of the sharp oscillations is roughly 3.5 ps, and corresponds to the vibrational frequency, ω. Notice that the Jaynes−Cummings curve exhibits no decay; in fact, over longer times it shows irregular aperiodic behavior.

2. Electronic dephasing: When electronic dephasing is added, the system does obtain an effective state density, and therefore shows irreversible decay to a final state.[39] This is seen in Figure 2a. The initial vibrational wave packet created on the excited surface of Figure 1 feels no nuclear dephasing or relaxation, and therefore the shape remains Gaussian. The system passes through the mixing region between the diabatic curves several times, and eventually transitions between the two electronic states occur. Because no vibrational relaxation is allowed, however, the system cannot exchange energy with its environment. Since the state density for the original photoexcitation energy in this very simple model is the same in either electronic state, the system does not relax to the bottom of the left well, that we will call V_L. Instead the asymptotics of the decay curves in Figure 2a proceed to an equal mixture of density on the left and right wells—that is, to a situation in which the charge transfer is only 50% complete. This result is unphysical for any real charge-transfer system.

3. Nuclear dephasing: When nuclear dephasing is permitted, the wave packet loses its initial Gaussian form, and eventually becomes spread over the entire vibrational coordinate of V_R. On the basis of Franck−Condon arguments, this suggests that the vibrational dephasing smooths the probability for the vibrational packet to be in the crossing region, and therefore gives smooth population transfer. Figure 2b shows the short time behavior as vibrational dephasing is increased. Note that the oscillations in the Jaynes−Cummings model indeed disappear very quickly, and that a smooth approach to equilibrium is found. Once again, because no vibrational relaxation is permitted, state densities in our one-mode model are the same in the two electronic states; asymptotic behavior and rate type kinetics occur, but the final state is not that of ordinary electron-transfer reactions.

4. Nuclear relaxation: Nuclear relaxation permits the system to transfer energy, and therefore to approach equilibrium. Figure 2c shows the effect of adding nuclear relaxation. Notice that the behavior is slightly complicated: for small nuclear relaxations, some of the Jaynes−Cummings model behavior is retained. The short time oscillations corresponding to the frequency of the tunneling matrix element remain, but asymptotic behavior is clearly seen. (In fact, there are also even shorter

(79) Jaynes, E. T.; Cummings, F. W. *Proc. IEEE* **1963**, *51*, 89.

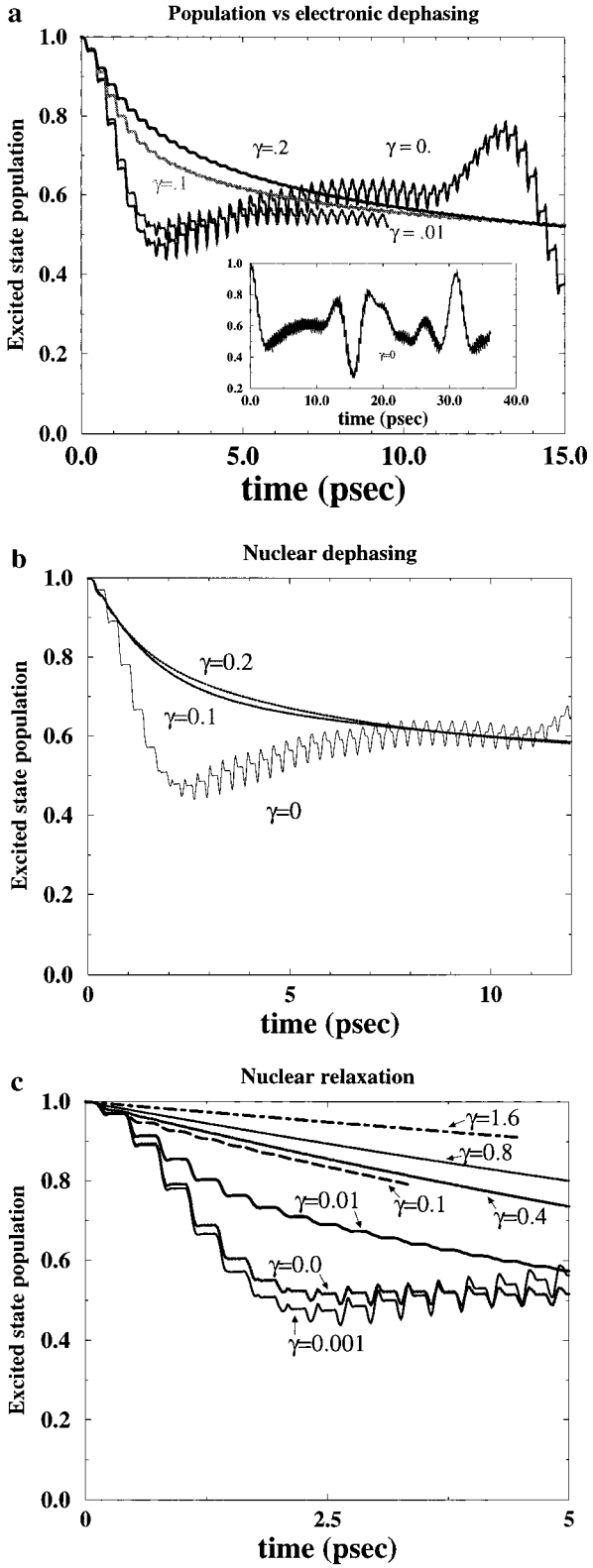

Figure 2. The decay of the initially excited population, with only one dissipative term (electronic or nuclear dephasing or nuclear relaxation). For no dephasing, the multiple oscillations are those of the Jaynes−Cummings model (Figure 2a, insert); with larger electronic dephasings (Figure 2a) or nuclear dephasings (Figure 2b), rate-like behavior is observed (although for the results in (a) or (b), showing results of increases in γ_{ed} and γ_{nd}, respectively, the asymptotic value of the excited-state population is 0.5). For increase in γ_{nr} (part c), the very short-time decay is slower, but a true rate process is seen. Parameter values are $J = 0.2\hbar\omega$, $\omega = 5.E{-}4$, $\Delta = -0.004$, $k_BT = 0.001$, $\gamma_{nr} = \gamma_{nd} = 0$. All energies are in hartrees (1 H = 27.21 eV).

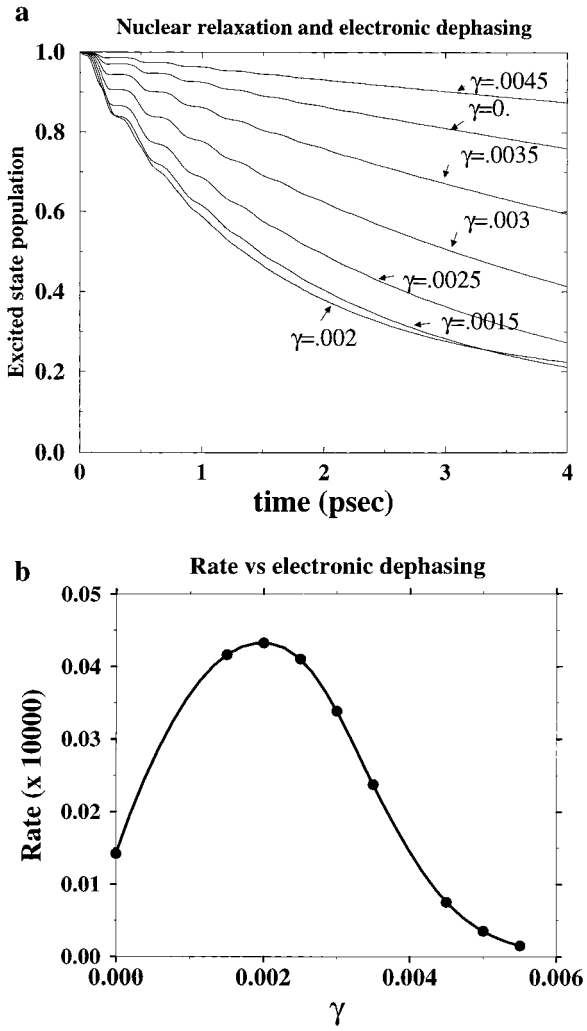

Figure 3. Behavior at short times as a function of increasing electronic dephasing, in the presence of nuclear relaxation. Part a shows nonmonotonic (turnover) behavior; for small γ_{ed}, the situation involves coherent transfer, whereas it becomes hopping for a large γ_{ed}. The turnover in rate constant is shown in part b. Parameters are the same as in Figure 2, except $\gamma_{nr} = 0.1$ and γ_{ed} is a variable.

time oscillations[42] that have the period $2\pi/\Delta$; these are irrelevant for our discussion.) As the relaxation amplitude becomes larger, eventually exceeding the tunneling matrix element, the kinetic behavior is slowed. This is the first indication of turnover behavior (discussed more extensively in Section IIIB).

5. Nuclear relaxation with electronic dephasing: Figure 3a shows the behavior in the presence of nuclear relaxation for increasing degrees of electronic dephasing. The behavior is now that expected for ET systems: the excited state population decays exponentially after a short period characterized by oscillations at the vibrational frequency. These oscillations, often called vibrational coherences, have been seen in several ultrafast studies, particularly in reaction centers.[24,80−82] The slopes (rate constants) are not monotonic in the electronic dephasing; again this is indicative of the onset of turnover behavior, to be discussed in Section IIIB.

6. Nuclear dephasing with nuclear relaxation: When both vibrational dephasing and vibrational relaxation are present, the effects of change in the nuclear dephasing rate are smaller than those shown in Figure 2b. This is because the total nuclear dephasing has contributions both from pure dephasing and from relaxation; this is familiar from magnetic resonance spectroscopy, and is generally expressed in terms of the longitudinal and transverse relaxation times, T_1, T_2, by[36,83]

$$\frac{1}{T_2} = \frac{1}{2T_1} + \frac{1}{T_2^*}$$

where T_2^* is the pure dephasing time (equal to $2\pi/\gamma_{nd}$ in our notation). The short time oscillations decrease with increasing vibrational dephasing, essentially for the Franck−Condon type reasons discussed above (the Gaussian packet on the vibrational state flattens out, so that the sharp oscillations arising from coherences are gone). Note that the rate is not simple exponential, but exhibits short time oscillations and long time slowing down. The reasons for the slow down at long time are depletion of the initial state and the fact that vibrational relaxation in the initial state eventually puts the packet at the bottom of V_R, where its transition to V_L is slowed.

B. Kinetics: Turnover Behavior. When nuclear relaxation is present, the decay of the initial state population (within V_R) eventually becomes irreversible and rate-like (Figures 2 and 3a). In this regime, the ET rate constant k_{ET} is well-defined. We study the variation of that rate constant with the system and bath parameters.

Kramers first pointed out,[84] in the context of the problem of classical escape over a potential energy barrier, that the effects of friction on chemical dynamics should be nonmonotonic: for low friction, the barrier escape rate should scale like friction, whereas for high friction scaling should be like inverse friction. Substantially more elaborate understandings of this behavior have since been produced,[85,86] but the essential physical argument is straightforward: for low frictions, energy cannot be transferred from the environment into the particle undergoing escape, whereas for very high frictions, the particle is simply slowed too much to pass over the top of the barrier. This turnover behavior is remarkably consistent in all analyses of the barrier passage problem.

In the current simple model, we observed several different forms of turnover behavior. Each of these can be understood physically, although they come in different categories, with the turnovers due respectively to relaxation phenomena, coherence phenomena, energetic phenomena, and state mixing.

1. Electronic dephasing turnover: Figure 3b shows the rate variation with electronic dephasing; parameters for this calculation are given in the caption. This turnover behavior as a function of electronic dephasing is reminiscent of the Kramers structure. It can be understood from extensive previous work on spin-boson type problems,[87] as well as analysis of exciton diffusion in molecular crystals.[88] Effectively, for very small electronic dephasing the process occurs coherently; an increase in dephasing magnitude provides an effective increase in state density. For large enough electronic dephasing, the coherent

(80) Diffey, W. M.; Homoelle, B. J.; Edington, M. D.; Beck, W. F. *J. Phys. Chem.* In press.
(81) Chachisvilis, M.; Pullerits, T.; Jones, M. R.; Hunter, C. N.; Sundstrom, V. *Chem. Phys. Lett.* **1994**, *224*, 345.
(82) Kumble, R.; Palese, S.; Visschers, R. W.; Dutton, D. L.; Hochstrasser, R. M. *Chem. Phys. Lett.* **1996**, *261*, 396.
(83) Laird, B. B.; Budimir, J.; Skinner, J. L. *J. Chem. Phys.* **1991**, *94*, 4391.
(84) Kramers, H. A. *Physica* **1940**, *7*, 284.
(85) Nitzan, A. *Adv. Chem, Phys.* **1988**, *70*, 489. Grote, R.; Hynes, J. T. *J. Chem. Phys.* **1982**, *77*, 3736.
(86) Fleming, G.; Hanggi, P., Eds. *Activated Barrier Crossing*; World: Singapore, 1993.
(87) Caldeira, A. O.; Leggett, A. J. *Physica A* **1983**, *121*, 587.
(88) Silbey, R. *Annu. Rev. Phys. Chem.* **1976**, *27*, 203. Suarez, A.; Silbey, R.; Oppenheim, I. *J. Chem. Phys.* **1992**, *97*, 5101.

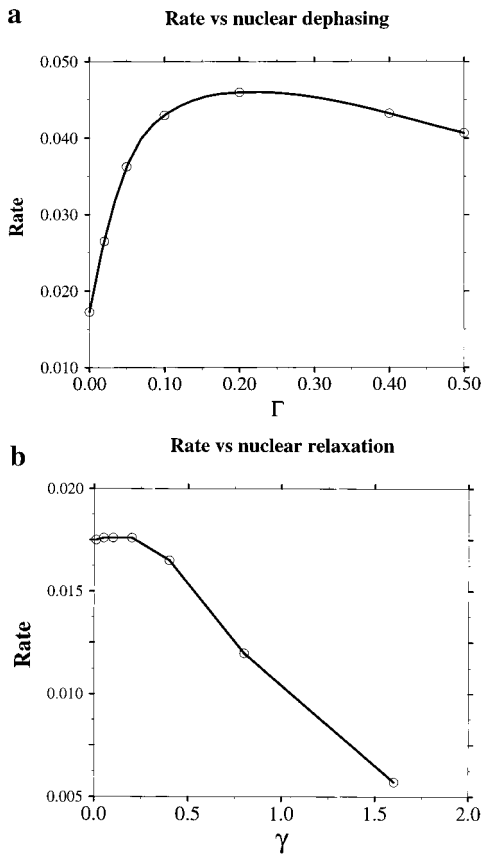

Figure 4. Weak turnover as a function of nuclear dephasing and relaxation. Parameter values as in Figure 3.

transport competes with incoherent diffusion, which becomes dominant at high enough values of the friction.

2. Nuclear dephasing turnover: Figure 4a shows the rate of transfer from V_R to V_L with increase of vibrational dephasing. Once again a maximum is observed, this time for a larger value of the dephasing amplitude. Once again, interpretation of the rising curve as due to effective increase of state density is appropriate, and coherent behavior becomes incoherent for large enough dephasing. For very large dephasing, the resonant condition required for energy sharing is hard to achieve, due to poor energy level fluctuation, and the rate drops off. Fundamentally, nuclear and electronic dephasing both correspond to energy level fluctuation, and they effect the ET rate similarly.

3. Nuclear relaxation turnover: As the rate of nuclear relaxation increases, when nuclear dephasing is present, the dominant behavior (Figure 4b) is a reduction in the rate (though a very weak turnover is again present). This can be understood simply by noting times at which the reduction begins. When the time for nuclear relaxation nears half the vibration period, energy will be lost from the excited-state vibrational motion before the crossing point of the two parabolas is reached. This means that the wave packet never quite reaches the Franck−Condon maximum for transition, so that the rate of the transitions drops. One would expect this effect to be less important at high temperatures. This behavior has been noted previously.[89]

4. Turnover in reorganization energy (Marcus inverted behavior):[55] When the displacement of the two parabolas, denoted as Q_0 in the Hamiltonian of eq 4, changes, the effective innersphere reorganization energy λ of eq 6 is modified. If the

(89) Schellenberg, P.; Loewe, R. J. W.; Shochat, S.; Gast, P.; Aartsma, T. J. *J. Phys. Chem.* **1997**, B101, 6786.

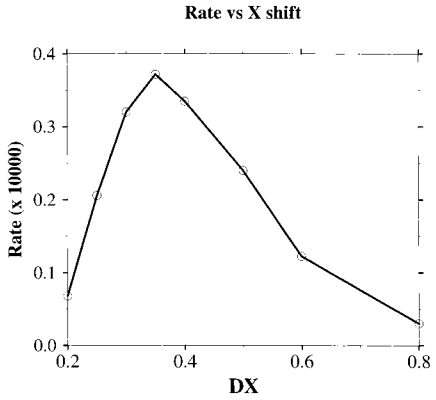

Figure 5. Rate as a function of the distance between abscissas for the two minima in the potential energy curves of Figure 1; the reorganization energy for the strongly coupled vibration, λ_i, is proportional to the square of this distance. Typical inverted region behavior is seen. Parameters are the same as in Figure 4.

transfer starts from the bottom of V_R, the barrier will vanish when the reorganization energy exactly balances the exoergicity. For further increase in Q_o, the rate drops as the system enters the inverted regime. This statement must be modified in two ways: first, we deal here with photoexcited transfer, rather than ground-state transfer, and the initial wave packet does not begin at the bottom of V_R. Second, the actual evolution is more accurately represented in terms of the adiabatic curves than the diabatic ones, and the barrier in the adiabatic curves is reduced compared to the diabatic barrier, by roughly J. For the parameters chosen here, the diabatic curves will cross for $Q_0 \cong 0.4$. The curve in Figure 5 shows that the maximum is indeed near 0.4 but is reduced slightly because of the photoexcitation and smoothing of the curve due to the mixing matrix element.

5. Turnover in electronic mixing: As the matrix element J increases, the appropriate interpretative picture goes smoothly from the diabatic behavior to the adiabatic one.[1,42] In particular, when J becomes very large, the effective adiabatic potentials are those shown in Figure 6a. In this case, photoexcitation produces a packet in the upper, quasiharmonic level. This packet will oscillate many many times before it drops to the ground adiabatic state. Therefore, as the matrix element J increases, one will first observe an increase in the rate (this is effectively the Golden Rule regime), with an eventual decrease because of the large gap that occurs in Figure 6a. This behavior is shown clearly in Figure 6b.

Thus we see that turnover behavior occurs as a function of electronic dephasing, vibrational relaxation, vibrational dephasing, exoergicity, and mixing matrix element. It is tempting to suggest that in systems of this type, with relatively small level densities, change of coupling conditions will as a general rule result in turnover behavior, since once the effective mixing becomes too strong, the appropriate uncoupled picture has changed—this is clearly what happens for the turnovers in electronic coupling and in electronic dephasing.

C. Long Time Behavior and Electron-Transfer Reaction Rate Constants. Starting with the initially photoexcited state, the system evolves substantially in phase space before it begins irreversible decay. Figure 7 shows the behavior with increase of the electronic tunneling parameter J. The very short time steps in Figure 7, like the steps seen previously, occur at intervals of the vibrational frequency; the steep falls then happen when the packet is near the crossing point between the two curves (this yields the vibrational coherences widely studied in the reaction center).[24,80−82] Figure 7 shows that for longer time

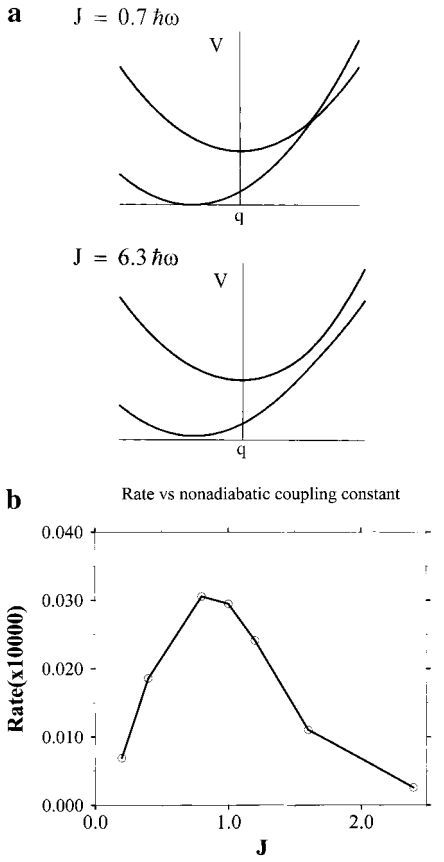

Figure 6. The behavior for large tunneling. Note that for large J values the upper adiabatic curve is far separated from the lower one (part a), causing turnover behavior corresponding to the transition from roughly diabatic to roughly adiabatic surfaces. Parameters are the same as in Figure 4, except for the variable tunneling parameter J.

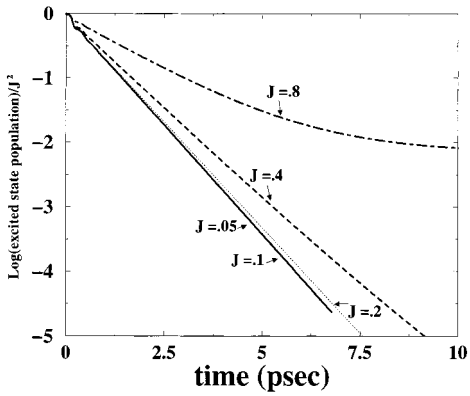

Figure 7. Test of the golden rule. The ordinate shows the logarithm of the excited-state population divided by J^2. Identical straight lines would be perfect Golden Rule behavior; the Golden Rule is really a very good approximation over this time scale. Parameters are the same as in Figure 4. The rate is in inverse atomic time units.

scales, the Golden Rule is almost but not quite obeyed: if the Golden Rule[72] were precise, the lines would all be straight and lie on top of one another. The slight differences arise from the fact that it is not actually the bare mixing matrix element (as suggested by the Golden Rule), but rather an effective matrix element that is more like a Rabi frequency, that in fact provides the mixing. Still, it is clear from this figure that for a fairly broad choice of mixing matrix elements, the Golden Rule approximation is quite good for time scales exceeding, say, 0.5 ps. The result for $J = 0.4\omega$ in Figure 7 does begin to stray from the Golden Rule prediction, since the diabatic picture is

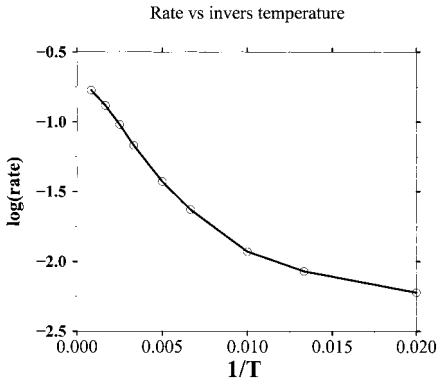

Figure 8. The rate constant as a function of inverse temperature. At high temperatures, activated behavior is seen. At low temperatures, nuclear tunneling dominates, and the behavior becomes only weakly temperature variant. Parameters are the same as in Figure 4.

becoming less reasonable; this is the start of the turnover behavior seen in Figure 6. For very long times, the Golden Rule again begins to break down. There are really two reasons for this breakdown: first is the depletion of the initial state, second is the vibrational relaxation in the reactant (right) well, which eventually leads to a slower rate constant, corresponding to tunneling through the barrier or overcoming the barrier, without the initial vibrational energy that was deposited by the vertical excitation. This suggests (in agreement with experiment)[89] that biexponential decay will be seen in photoexcited systems of this type, with the faster rate constant corresponding to the dynamics of the initially excited system and the slower rate constant corresponding to charge transfer from the relaxed, thermalized photoexcited state in V_R.

The temperature dependence of the rate constant in the first-order kinetic regime is essentially of Arrhenius type (Figure 8). At very low temperatures, one expects the rate to be effectively temperature independent, and to arise largely from tunneling contributions.[51−59,74] This is more exaggerated in the case of ET starting with no vibrational energy; in the current case, the initially deposited energy can cause transitions without extensive nuclear tunneling, simply because the packet uses initially deposited vibrational energy to approach the transition point; this could not occur with transfer starting from the bottom of V_R, and therefore the effective flatness of the curve at high temperatures is slightly reduced here compared to the other situation.

Figures 3a, 4a, and 5 all yield rate constants of the order 5×10^{11}/s.

There are two standard analyses of the rate problem defined by the Hamiltonian (1).[51−59] In the limit of purely classical behavior, Marcus derived the important result[55]

$$k_{et} = A \exp\{-(\lambda + \Delta_R)^2/4\lambda RT\} \qquad (11)$$

here, A is the prefactor depending on the nature of the coupling strength, and the Gaussian form arises from the assumptions of activated barrier crossing (characteristic of transition state theory) and of harmonic vibrations. In the original formulation, the reorganization energy λ included only the solvent reorganization; the simplest extension to include intramolecular vibrations is to replace this λ by the total reorganization energy, the sum of the reorganization energies for intramolecular vibrations and solvent reorganization. When nuclear tunneling processes are permitted, standard analysis due to a number of

workers,[91−94] particularly Jortner,[74] results in a polaron-like treatment that yields the rate constant in the form (with only one active vibration and λ_o the reorganization energy from the solvent and other classical modes):

$$k_{et} = A\sum e^{-s}\frac{S^{\nu}}{\nu!}\exp\left\{\frac{-[\lambda_o + \nu\hbar\omega + \Delta]^2}{4\lambda_o RT}\right\} \qquad (12)$$

For nonadiabatic transfer, the prefactor is given by

$$A = 2\pi J^2/\hbar[4\lambda k_B T]^{1/2} \qquad (13)$$

Here the sum runs over the states of the intramolecular vibration. The assumptions resulting in eq 12 are not particularly restrictive: in addition to the validity of the simple spin-boson form of eq 1, they include the assumption that the solvent modes can be treated as low-frequency vibrations whose frequencies are small compared to thermal energies, the existence of sufficiently strong relaxation and dephasing effects that the electron-transfer process occurs at equilibrium (there is no bottlenecking due to solvent relaxation), the assumption that the initial state has no vibrational quanta excited, and the overall validity of a rate constant (that is, relaxation and dephasing are strong enough that the vibrations can be discussed in terms of thermal equilibrium). All of these assumptions can become doubtful at very short times; indeed, such short time behavior is a major focus of our analysis here. For the choice of model parameters made here, the effective λ_o arises from the vibrational relaxation and dephasing. The λ_o can then be roughly estimated by equating half-widths of the line shapes given by the form of eq 12 with that coming from the simple broadening. This yields the form

$$\ln 2 = (2\pi\hbar/T_2 - \Delta - \lambda_o)^2/4\lambda_o k_B T \qquad (14)$$

IV. Comments

The model analyzed in this manuscript is to some extent an artificial one, because the Hamiltonian behavior is that of the Jaynes−Cummings model; this has no relaxation properties, and its effective state densities are constant both well below and well above the crossing regime. This latter situation will not hold in any realistic model of electron transfer, for which the vibrational state density will increase very rapidly with energy.

These state density effects are to some extent captured by dissipative terms that we have introduced. The model permits understanding of the effects of different dephasing, relaxation, mixing, and thermal properties, in an exact calculation (albeit of a very simplified model).

The model for the potential energy surfaces is the spin-boson one that is almost always used for the description of electron transfer (and of many other related phenomena). It actually has some inadequacies as a picture of system/bath coupling since (to some extent) it artifically overcorrelates the interaction.

There are several striking observations of the current study. In the short time dynamic regime that follows photoexcitation, the wave packet evolves on the upper state, and approaches the Franck−Condon transition region, where it effectively mixes with the lower state. The dynamical behavior is characterized by coherences and resonances—no reversible kinetics occurs.

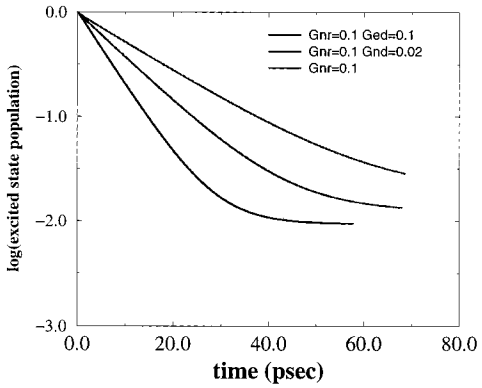

Figure 9. The biexponential dependence of the rate on time, with strong nuclear relaxation terms. The short time rate is dominated by transfer with the initially deposited energy in the strongly coupled mode. Nuclear relaxation causes decay to the bottom of V_R, from which nuclear tunneling is necessary to produce rate-type behavior.

The onset of irreversible kinetics is fixed by the magnitude of dephasing or relaxation. Vibrational relaxation permits the system to decay away from the original vibrational energy content, and, thereby, to be trapped on the left potential curve, without the possibility of effective re-crossing. This gives relaxation and rate constant behavior. The vibrational dephasing facilitates transfer by increasing density at the curve crossing point, and also prohibits recrossings for time substantially longer than the inverse of the dephasing amplitude. Finally, electronic dephasing removes the coherences, so that the transition is characterized by a hopping process that is effectively irreversible in this system for which the product curve has lower electronic energy than the reactant.

After irreversible kinetics has begun, one can characterize the rate constant in terms of the parameters of the system. We observe Golden Rule like behavior even for very large values of the mixing matrix element, *J* (Figure 7b). This is unexpected on the basis of polaron analysis with degenerate donor and acceptor states, but is reasonable when the exoergicity becomes large compared to the vibrational frequency, and is essentially required in the inverted region.

For sufficiently large vibrational relaxation and small *J*, the kinetic behavior is effectively of double-exponential type. At short times, such that $\gamma_{nr}t < \pi$, the curve crossing is dominated by the energy content imparted by the initial photoexcitation. For the choice of reorganization energy that we have made (motivated by experimental work on mixed valent systems),[8,10,20,25] this is adequate to permit the wave packet to reach the crossing region without nuclear tunneling, and therefore the rate is relatively fast, of order 5×10^{11}/s. For later times, $\gamma_{nr}t \gg \pi$, the density remaining on V_R has largely relaxed to the bottom of this well, and the remaining rate constant is far smaller ($\sim 10^{10}$/s), as predicted by polaron-type rate theories (Figure 9).

There is striking turnover behavior: the rate constant exhibits turnover behavior as a function of electronic dephasing, nuclear dephasing, nuclear relaxation, mixing matrix element, and reorganization energy. These inversions occur for different reasons: the behaviors with increasing dephasing magnitude are indicative of a change in mechanism, while the turnaround in reorganization energy arises from minimization, and then regrowth, of an effective barrier on the potential energy surface (Marcus inverted behavior),[55] and the turnaround in mixing matrix element arises because of the nature of the crossing transition. Nevertheless, the fact that five different turnover behaviors occur in this very simple model suggests that turnover behavior of this kind may be found not only in the Marcus

(90) Wegewijs, B.; Scherer, T.; Rettschnick, R. P. H.; Verhoeven, J. W. *Chem. Phys. Lett.* **1993**, *176*, 349.
(91) Fischer, S. F.; Duyne, R. P. V. *Chem. Phys.* **1977**, *26*, 9.
(92) Hopfield, J. J. *PNAS* **1974**, *71*, 3640.
(93) Scher, H.; Holstein, T. *Philos. Mag. B* **1981**, *44*, 346.
(94) Schmidt, P. P. *Electrochem. Spec. Period. Rep.* **1978**, *6*, 128.

inverted regime and in Kramers-like barrier crossings, but also in true quantal charge dynamics.

Three experimental behaviors are suggested by these calculations, involving the short-time dynamics, turnover behavior, and biexponential decay.

Experimentally, dephasing behaviors have been studied extensively in a number of molecular systems, particularly the multiple coupled pigments of the photosynthetic reaction center.[15] Several experimental analyses have indeed pointed to some of the effects observed in these calculations, including the pump−probe spectroscopic observation of vibrational coherences, dephasing and relaxation times, and correlation of dephasing behavior with the onset of rate phenomena.

Biexponential decay has also been observed in several situations, and the explanation given[89] was essentially the competition between curve crossing and initial state relaxation that we observe here.

The other striking observation from the current discussion is the general appearance of turnover behavior: turnovers in mixing matrix element have not really been characterized, but at some levels they simply correspond to redefinition of the unperturbed state, from the nonadiabatic to the adiabatic limits. They are important for several reasons: in particular, they demonstrate that the Golden Rule result $k \sim J^2$ will fail badly (in the kinetic regime) for sufficiently large J. It will be of interest to test, both experimentally and in more general model calculations with several active modes and with mode anharmonicity, how general these turnover behaviors will be.

Acknowledgment. M.R. is grateful to the Chemistry Division of the NSF and to the DOD-MURI program for support. The Fritz Haber Institute is partly supported by the Minerva Gesellschaft fur die Forschung, München. We thank Paul Barbara, Norbert Scherer, and Abe Nitzan for valuable remarks and the referee of an initial version for very helpful comments.

Appendix 1. Parameter Values

The behavior of the photoexcited state is described by the hamiltonian parameters ω, Δ, Q_o, M, and J, plus the relaxation parameters γ_{nr}, γ_{nd}, and γ_{ed}, and the temperature T.

For the hamiltonian, we chose parameters suggested by the mixed-valence system[10] $(NH_3)_5RuNCRu(CN)_5^-$: $Q_o = 0.106$ Å, $-\Delta = 0.109$ eV, $\omega = 110$ cm^{-1}, $M = 20$ dalton, $J = 0.2\ \hbar\omega$. The default values for the relaxation parameters are $\gamma_{ed} = \gamma_{nr} = \gamma_{nd} = 0.2\hbar\omega$.

JA981998P